Enhancement of endogenous midbrain neurogenesis by microneurotrophin BNN-20 after neural progenitor grafting in a mouse model of nigral degeneration

Theodora Mourtzi[1, *], Nasia Antoniou[2, #], Christina Dimitriou[1, #], Panagiotis Gkaravelas[2, #], Georgia Athanasopoulou[2], Panagiota Nti Kostantzo[1], Olga Stathi[1], Efthymia Theodorou[1], Maria Anesti[1], Rebecca Matsas[2], Fevronia Angelatou[3], Georgia Kouroupi[2, §], Ilias Kazanis[1, *, §]

From the Contents

Graphical Abstract

BNN-20 leads to partial amelioration of the pathological phenotype of PD iPSCs-derived neurons and a strong appearance of an endogenous neuroblast cluster in the NSPC-grafted adult midbrain
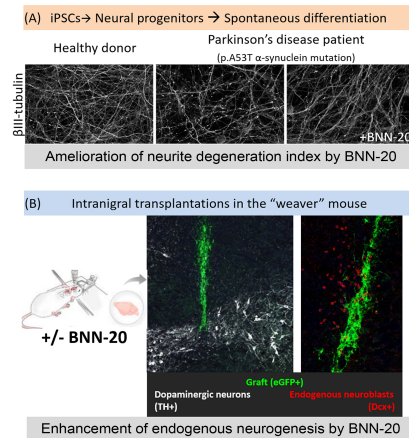
Abstract

We have previously shown the neuroprotective and pro-neurogenic activity of microneurotrophin BNN-20 in the substantia nigra of the "weaver" mouse, a model of progressive nigrostriatal degeneration. Here, we extended our investigation in two clinically-relevant ways. First, we assessed the effects of BNN-20 on human induced pluripotent stem cell-derived neural progenitor cells and neurons derived from healthy and parkinsonian donors. Second, we assessed if BNN-20 can boost the outcome of mouse neural progenitor cell intranigral transplantations in weaver mice, at late stages of degeneration. We found that BNN-20 has limited direct effects on cultured human induced pluripotent stem cell-derived neural progenitor cells, marginally enhancing their differentiation towards neurons and partially reversing the pathological phenotype of dopaminergic neurons generated from parkinsonian donors. In agreement, we found no effects of BNN-20 on the mouse neural progenitor cells grafted in the substantia nigra of weaver mice. However, the graft strongly induced an endogenous neurogenic response throughout the midbrain, which was significantly enhanced by the administration of microneurotrophin BNN-20. Our results provide straightforward evidence of the existence of an endogenous midbrain neurogenic system that can be specifically strengthened by BNN-20. Interestingly, the lack of major similar activity on cultured human induced pluripotent stem cell-derived neural progenitors and their progeny reveals the *in vivo* specificity of the aforementioned pro-neurogenic effect.

Key Words: adult neurogenesis; BNN-20; brain-derived neurotrophic factor; cell replacement; induced pluripotent stem cells (iPSCs); neurotrophic factors; Parkinson's disease; substantia

Introduction

Cell replacement therapies (CRTs) have been investigated intensely as possible treatments for neurodegenerative disorders, with Parkinson's disease (PD), which is characterized by the specific loss of dopaminergic neurons in the substantia nigra pars compacta (SNpc), being a suitable target. CRTs can be based on cell transplantations, or the pharmacological recruitment of endogenous brain neural progenitors (Mourtzi and Kazanis, 2022). An alternative strategy could involve the administration of neurotrophins/neurotrophic factors, on their own or as CRT complements (Mendez et al., 2000; Marsh and Blurton-Jones, 2017). Such molecules enhance the viability, differentiation, and branching of grafted cells, and/or stimulate endogenous neurogenesis (Marsh and Blurton-Jones, 2017; Mourtzi and Kazanis, 2022).

Previous results have shown that the synthetic microneurotrophin BNN-20 exhibits strong neuroprotective and pro-neurogenic activity in the SNpc of the "weaver" mouse, a model of progressive nigrostriatal degeneration (Botsakis et al., 2017; Panagiotakopoulou et al., 2020; Mourtzi et al., 2021). BNN-20 acts as a micromolecular mimetic of BDNF, exerting strong antioxidant, anti-inflammatory and neuroprotective properties (Botsakis et al., 2017; Panagiotakopoulou et al., 2020), enhancing endogenous dopaminergic neurogenesis specifically in the SNpc (Mourtzi et al., 2021), and leading to behavioral improvement (Panagiotakopoulou et al., 2020). Here, we extend the investigation in two more clinically-relevant ways. Firstly, we assess the effects of BNN-20 on human induced pluripotent stem cell (iPSC)-derived neural progenitor cells (NPCs) and neurons, generated from healthy and parkinsonian donors. Secondly, we assess if BNN-20 can boost the outcome of NPC transplantations in the weaver SNpc. Since BNN-20 promotes endogenous mouse neurogenesis and induces the differentiation of mouse NPCs *in vitro*, we hypothesized that its administration, before and after grafting, could exert a cumulative positive effect.

[1]Laboratory of Developmental Biology, Department of Biology, University of Patras, Patras, Greece; [2]Laboratory of Cellular and Molecular Neurobiology-Stem Cells, Hellenic Pasteur Institute, Athens, Greece; [3]Department of Physiology, School of Medicine, University of Patras, Patras, Greece
*Correspondence to: Ilias Kazanis, MSc, PhD, ikazanis@upatras.gr; Theodora Mourtzi, MSc, PhD, mourtzi@upatras.gr.
https://orcid.org/0000-0003-1035-0584 (Ilias Kazanis); https://orcid.org/0000-0001-5106-8214 (Theodora Mourtzi)
#These authors contributed equally to this paper.
§Both authors share the senior authorship of this paper.

Methods

Ethics statement
Animal breeding, maintenance, and handling were performed in accordance with the European Communities Council Directive Guidelines (86/609/EEC) for the care and use of Laboratory animals as implemented in Greece by the Presidential Decree 56/2013 and approved and scrutinized by the Western Greece Prefectural Animal Care and Use Committee (approval No. 109724/403, approval date: May 21, 2020). This study was reported in accordance with the ARRIVE 2.0 guidelines (Animal Research: Reporting of *In Vivo* Experiments) (Percie du Sert et al., 2020).

Animals
Male and female homozygous "weaver" (Aw-J/A-Kcnj6wv/J) mice (a genetic model of progressive nigrostriatal degeneration) of the B6CBAC strain and age-matched B6CBAC wild-type controls, inbred at the designated animal facilities of the University of Patras (EL13 BIOexp-04) were used. For the transplantation of NPCs, we used five C57BL/6-Tg(CAG-EGFP)1Osb/J transgenic mice of both genders (Jackson Laboratory, Bar Harbor, ME, USA, Stock No. 003291, RRID: IMSR_JAX:003291), universally expressing eGFP, aged 2–4 months (provided by Jackson Laboratory and inbred at the designated animal facility of the Hellenic Pasteur Institute). Their body weight was age-appropriate, and their health status was good as they did not exhibit any signs of disease. The mice used for all experiments were naive. Animals were maintained in a steady light/dark cycle (12/12 hours) with free access to food and water, at a maximum number of four animals per cage. Identification of homozygotes (referred to as "weaver" or wv) was based on their smaller size and well-described motor and behavioral traits, including weakness, hypotonia, extensive periods of resting and movement-initiated tremor, poor limb coordination, and instability of gait (Hirano and Dembitzer, 1973). They had access to a paste consisting of standard rodent food pellets and water, as they are unable to reach the water bottles, due to their limited mobility.

iPSCs
Human iPSCs and iPSC-derived NPCs were generated from skin fibroblasts derived from a PD patient carrying the G209A (p.A53T) SNCA (α-synuclein gene) mutation and a healthy individual as previously reported (Kouroupi et al., 2017). Skin fibroblasts were obtained from the Biobank generated within the context of the European Project on Mendelian Forms of Parkinson's Disease (MEFOPA; https://www.mefopa.eu/Subproject3.html). All procedures for generation of human iPSCs were approved by the Scientific Council and Ethics Committee of Attikon University Hospital (Athens, Greece), which is one of the Mendelian forms of Parkinson's Disease clinical centers, and by the Hellenic Pasteur Institute Ethics Committee overlooking stem cell research, in 02/05/2011. However, the human iPSCs and iPSC-derivatives used for the present study have already been generated, characterized and used as described in the study by Kouroupi et al. (2017), so the information regarding informed consent was not needed here.

iPSC-derived NPCs were derived as previously described (Kouroupi et al., 2017), following a neural induction protocol based on dual-SMAD inhibition (Chambers et al., 2009). NPCs were either expanded in STEMdiff Neural Progenitor Medium (STEMCELL Technologies, Vancouver, BC, Canada) or differentiated into neurons (**Figure 1**; more details on the protocols are provided in **Additional file 1**). For spontaneous differentiation, NPCs were cultured for 10–15 days *in vitro* (DIV) and then were analyzed by immunocytochemistry or harvested for RNA extraction and quantitative reverse transcription-polymerase chain reaction (qRT-PCR).

BNN-20 treatment of human iPSC-derived neuronal cultures
Microneurotrophin BNN-20 (Bionature E.A. Ltd, Nicosia, Cyprus) was resuspended in pure ethanol in a 10^{-2} M concentration. This solution was then diluted in sterile PBS (10^{-4}) and finally, in the cell culture medium at a final concentration of 10^{-7} M. Control and PD-derived NPCs and differentiated neurons were cultured in the presence of BNN-20 for up to 2 weeks as described in **Figure 1A**.

NSC^{eGFP} cultures and graft preparation
For NPC cultures, the mice were killed by cervical dislocation after sedation via an intraperitoneal (i.p.) injection of 100 mg/kg ketamine (Ketamidor, 100 mg/mL, Richter Pharma AG) and 10 mg/kg xylazine (Rompun, 2% w/v, Bayer, St. Louis, MO, USA), and the subependymal zones were dissected under the stereoscope using anatomical landmarks, as performed previously (Mourtzi et al., 2021). They were then dissociated using accutase, and resuspended in NPC proliferation medium consisting of high glucose DMEM (Gibco DMEM, Thermo Fisher Scientific, Waltham, MA, USA, Cat# 11965092), FGF2 (Peprotech, Cat# 100-18B) and EGF (Peprotech, AF-100-15) at 20 ng/mL, B27 (Thermo Fisher Scientific, Cat# 11965-084) and N2 supplements (Thermo Fisher Scientific, Cat# 11965-084) and grown as 3D free-floating aggregates called neurospheres that were passaged up to 8 times before grafting. The expression of eGFP was confirmed in using confocal microscopy (Leica TCS SP8, Leica, Wetzlar, Germany). The day prior to the transplantation, neurospheres were dissociated and the density of live cells was quantified after trypan blue staining. On the day of transplantation, the cells were centrifuged (800 × *g*, 10 minutes), resuspended to achieve the desired concentration for grafting in proliferation medium (200,000 live cells per 2.5 µL of cell suspension), and kept at room temperature for a maximum of 3 hours, until grafting.

Stereotaxic surgery for cell transplantations and administration of BNN-20
Animals (at postnatal days (P)45) were maintained under anesthesia via inhalation of isoflurane (Dechra Pharmaceuticals, Northwich, England; 3% v/v for induction until loss of limb reflexes and 2% v/v for maintenance) and were placed on a stereotaxic frame. Cells were resuspended by gentle pipetting immediately before engraftment and were injected in the brain using a 10 µL Hamilton syringe at the following coordinates: AP: –0.36 cm, ML: +0.1 cm, Z: –0.35 mm, based on the criteria of Paxinos and Franklin (2013). The cell suspension (or suspension medium only, for sham controls) was injected slowly 1 µL/min, with a 30-second pause after each 0.5 µL). At the end the needle was retrieved for 0.2 mm and was left in the tissue for another 5 minutes, to allow the graft to settle. BNN-20 (1 mg/mL in 4% v/v ethanol, 0.9% NaCl) (Bionature E.A. Ltd, Nicosia, Cyprus) or same volume of vehicle (4% v/v ethanol in 0.9% NaCl solution) was administered to the graft-receiving animals via i.p. injection daily (100 mg BNN-20 per kg b.w.), during P30–P60. For further information on the exact timeline of those interventions, see **Additional Figure 1**.

Immunofluorescence
iPSCs-derived and neurosphere cells were fixed with 4% and 2% paraformaldehyde (Sigma-Aldrich, St. Louis, MO, USA), respectively. They were immunostained at 4°C overnight with the primary antibodies listed in **Additional file 1**, followed by incubation with appropriate secondary antibodies. Images were acquired using confocal microscopy (Leica TCS SP8) and analyzed using ImageJ software (Java 8; National Institutes of Health, Bethesda, MD, USA; Schneider et al., 2012). For the *in vitro* assessment of the NSCseGFP neurospheres (passages 5–8) were subjected to a 5-day *in vitro* differentiation protocol, by growth factor withdrawal.

For tissue analysis, all animals (control and "weaver" were placed under anesthesia using an intraperitoneal injection of 100 mg/kg ketamine (Ketamidor, 100 mg/mL, Richter Pharma AG) and 10 mg/kg xylazine (Rompun, 2% w/v, Bayer, St. Louis, MO, USA) and intracardially perfused with 20 mL normal saline solution followed by 20 mL paraformaldehyde 4% w/v (Sigma-Aldrich, Cat# 158127) for tissue fixation. The brains were post-fixed overnight at 4°C and were frozen. Cryostat tissue sections (14 µm) were processed for antigen retrieval, when necessary, and incubated with primary antibodies (**Additional file 1**) and the appropriate secondary antibodies. Images were obtained by confocal (Leica TCS SP8) microscopy, using the 40× and 63× objectives, and saved in a high-resolution ".tiff" format. Quantifications were performed using the LasX software (Leica Microsystems, Wetzlar, Germany). For the cell-type profile analysis of the graft, all sections including grafted cells were imaged, taking two optical fields at the right and the left side of the graft along its dorsoventral tract. For the cell-type analysis in the SNpc, images of at least six random optical fields were taken from each area of both hemispheres, from at least two brain sections per animal. In the absence of TH immunostaining, the SNpc was identified using anatomical landmarks and adjacent sections stained for TH.

Total dopaminergic neuron quantifications in the SNpc
The total number of dopaminergic neurons of the SNpc was evaluated by immunofluorescence staining for the tyrosine hydroxylase (TH) dopaminergic cell marker. Images were obtained with the 20× objective by confocal (Leica TCS SP8) microscopy. The SNpc was determined based on the stereotaxic coordinates of Paxinos and Franklin (2013). The total TH$^+$ cell number of the SNpc was quantified stereologically: all TH$^+$ cells were counted in both hemispheres in 10 equally distanced sections (100 µm step) in each animal (*n* = 4 per group). The total dopaminergic cell number was determined using the following formula, appropriate for stereological cell quantification (Ellis et al., 2004) as performed previously (Mine et al., 2013; Simões et al., 2022):

Number of neurons = 1/ssf (slice sample fraction) × 1/asf (area sample fraction) × 1/tsf (thickness sampling fraction) × number of objects counted

qRT-PCR
Total RNA was extracted from control and PD iPSC-derived neuron pellets using TRIzol Reagent (Thermo Fisher Scientific). RNA concentration was measured on NanoDrop One Spectrophotometer (Thermo Fisher Scientific). Following digestion with DNase I (Promega, Madison, WI, USA), 1–1.5 µg of total RNA was used for first-strand cDNA synthesis with the ImProm-II Reverse Transcription System (Promega) following the manufacturer's protocol. Quantitative PCR analyses were conducted in a Light Cycler96 (Roche, Basel, Switzerland) Real-time PCR detection system using SYBR Select Master Mix (Thermo Fisher Scientific) according to the manufacturer's instructions. All primers used are listed in **Additional file 1**.

For quantitative reverse transcription-polymerase chain reaction (qRT-PCR) analysis we used SYBR Select Master Mix (Thermo Fisher Scientific) according to manufacturer's instructions. In particular, the qRT-PCR conditions were as follows: 95°C for 2 minutes denaturation, followed by 40 cycles of 95°C for 15 seconds, and 60°C for 60 seconds.

Results were analyzed using the ΔCt method ($2^{-\Delta\Delta Ct}$) (Schmittgen and Livak, 2008). The reference gene glyceraldehyde-3-phosphate dehydrogenase (GAPDH) was used in comparisons of gene expression data.

The primers (5'–3') used are the following: GAPDH, forward: CCT CTG ACT TCA ACA GCG ACA C, reverse: AGC CAA ATT CGT TGT CAT ACC AG; MAP2, forward: GAG AAT GGG ATC AAC GGA GA, reverse: CTG CTA CAG CCT CAG CAG TG; βIII tubulin (TUJ1), forward: CAT TCT GGT GGA CCT GGA AC, reverse: CCT CCG TGT AGT GAC CCT TG; SNCA, forward: GGA GTG GCC ATT CGA CGA C, reverse: CCT GCT GCT TCT GCC ACA C; TRKB, forward: ACA GTC AGC TCA AGC CAG ACA C, reverse: GTC CTG CTC AGG ACA GAG GTT A.

Neurite analysis

Neurite analysis was performed on either DsRed-labeled or TH[+] iPSC-derived dopaminergic neurons at 25 DIV. A lentiviral vector expressing the red fluorescent protein (DsRed) under the control of the human synapsin 1 promoter (LV.SYN1.DsRed) was used for the transduction of human cells to facilitate imaging of single neurons for morphological analysis (Kouroupi et al., 2017). Transduction with LV.SYN1.DsRed was performed at least 7 days before the assay to depict and count branching neurites from single neurons. The number of neurites extending from the soma of at least 100 single DsRed-labeled neurons per sample was determined. Neurite length was estimated by manually tracing the length of all neurites on DsRed-labelled neurons using the NeuronJ plugin of ImageJ. For morphological analysis of iPSC-derived dopaminergic neurons, at least 50 TH^{+} neurons were assessed for the number of neurites and the total neurite length.

Neurite degeneration index

Analysis of neurite degeneration was performed using ImageJ after immunostaining for βIII-tubulin (TUJ1). The number of TUJ1^{+} spots in fragmented neurites was manually counted on ten randomly selected fields. We then calculated the ratio between the number of spots and the total TUJ1^{+} staining area. This ratio divided by its respective control was defined as neurite degeneration index (NDI; in control conditions the index was 1).

Statistical analysis

All data are given as the mean ± standard error of the mean (SEM). Statistical analysis was performed using Microsoft Excel (Microsoft Corporation, 2018; Microsoft, Redmond, WA, USA), GraphPad Prism version 6.00 for Windows (GraphPad Software, San Diego, CA, USA, www.graphpad.com), and SPSS Statistics 25 (IBM, Armonk, NY, USA). Comparisons between two independent groups were performed using Student's t-test. One-way or two-way analysis of variance with Tukey's $post\ hoc$ test, least significant difference $post\ hoc$ test, or Bonferroni correction, was applied for multiple group comparisons. Pearson's correlation analysis was performed to evaluate if there is a correlation between the number of graft-derived (eGFP[+]/Dcx[+]) and endogenous (eGFP[−]/Dcx[+]) neuroblasts with the total number of grafted (eGFP^{+}) cells. Probability values less than 0.05 were considered significant.

Results

BNN-20 marginally improves the degenerative index of neurons in a human iPSC-based model of Parkinson's disease

Human NPCs are a potential source of cells for CRTs, but also a valid experimental system to model PD; thus, we investigated the effects of BNN-20 on these cells derived either from healthy or parkinsonian donors carrying the p.A53T α-synuclein mutation (G209A in the SNCA gene) (Kouroupi et al., 2017). Both control and PD iPSC-derived NPC cultures expressed Nestin and Pax6 with no significant differences between them (data not shown; Kouroupi et al., 2017). NPCs were allowed to differentiate spontaneously into βIII-tubulin-expressing (TUJ1^{+}) neurons for two weeks (**Figure 1A**, **B**, and **D**). α-Synuclein (αSyn) protein was present in the soma and neurites of both PD and control iPSC-derived neurons, though more cells were strongly positive for αSyn in PD cultures (**Figure 1B**) and levels of αSyn mRNA were significantly higher in PD cultures ($P < 0.05$; **Figure 1C**).

After confirming the expression of TrkB neurotrophin receptor, through which BNN-20 acts $in\ vivo$ (Botsakis et al., 2017; **Figure 1E**), we cultured control and PD iPSC-derived NPCs under spontaneous neuronal differentiation conditions, with or without BNN-20, for up to 25 DIV (**Figure 1A**). Although Qrt-PCR analysis did not reveal significant differences between control, PD and BNN-20-treated cultures, slightly increased, but not statistically significant, number of TUJ1^{+} neurons was observed in PD cultures after BNN-20 treatment ($P = 0.056$; **Figure 1F–K**).

Subsequently, we assessed the effects of BNN-20 on disease-associated phenotypes of PD cultures. Upon differentiation, PD iPSC-derived neurons exhibit degeneration traits exemplified by contorted or fragmented TUJ1^{+} neurites, displaying αSyn[+] swollen varicosities and large spheroid inclusions, similar to the dystrophic neurites of p.A53T patients (Duda et al., 2002; Kouroupi et al., 2017). Here, we identified TUJ1^{+} fragmented axons at the second week of neuronal differentiation (NDI, Control $vs.$ PD, P=0.019; **Figure 2A** and **B**). Moreover, after lentiviral expression of DsRed in a concentration enabling us to label single neurons, we found that the average neurite length was reduced -but not significantly- in PD neurons (Control $vs.$ PD, $P = 0.098$; **Figure 2C** and **D**) as was the total number of neurites extending from the soma (Control $vs.$ PD, $P = 0.106$; **Figure 2E**). Neurons differentiated in the presence of BNN-20 were partially protected, particularly with respect to degeneration as their DI was not significantly different from that of control cells ($P < 0.05$; **Figure 2B**). Yet, impaired neurite length and branching were not restored by BNN-20 in either the neuronal population (**Figure 2C–E**) or, more specifically, in TH^{+} dopaminergic neurons (**Figure 2F–H**; control $vs.$ PD, $P < 0.05$; one-way analysis of variance).

Transplantations of mouse NPCs[eGFP] in the SNpc of the weaver mouse

Previously published data (Mourtzi et al., 2021) suggested that BNN-20 exhibits neurogenic and neuroprotective effects on endogenous NPCs when administered $in\ vivo$ in the weaver mouse, yet our present data on human iPSC-derived cells suggested more limited outcomes when acting directly on NPCs $in\ vitro$. To investigate this further, we performed transplantation experiments in weaver mice as a unique opportunity to monitor and assess,

simultaneously, the effects of BNN-20 on grafted (exogenous) and on the host's (endogenous) NPCs.

Adult eGFP-expressing progenitors (NPCs[eGFP]) were isolated and expanded in culture from the brain of C57BL/6-Tg (CAG-eGFP)1Osb/J mice. Initially, we cultured NPC[eGFP] from two separate mouse lines to assess: i) the differentiation potential between separate lines, ii) the persistence and pattern of eGFP expression in differentiated cells, and iii) whether immunofluorescent staining was necessary for the detection of eGFP. We assessed eGFP expression after 5 days of $in\ vitro$ differentiation in neurons (immunopositive for β-III tubulin and Doublecortin/[Dcx]) and astrocytes (immunopositive for glial fibrillary acidic protein [GFAP]) (**Additional Figure 2A**). No significant differences were observed between the two lines regarding the percentage of cells expressing eGFP (data not shown) and their capability to differentiate towards neurons and astrocytes (**Additional Figure 2C**). Therefore, we considered NPCs[eGFP] generated from different lines as a homogeneous population that could be used interchangeably or pooled together. eGFP was detected in the vast majority of cells (~98.6%), as expected by the ubiquitous expression of the transgene. Nevertheless, its detection was significantly improved after immunofluorescence staining against eGFP (increased to ~99.8% of cells, $p <$ 0.05 using Student's t-test) (**Additional Figure 2B**); thus, we decided to apply anti-eGFP immunostaining to all of our further $in\ vivo$ and $in\ vitro$ analyses.

Because the intended use of NPCs[eGFP] was the detection of graft-generated neurons within the SNpc, we also assessed the expression of eGFP in Dcx[+], β-III tubulin[+], and GFAP^{+} cells. We detected eGFP in the nucleus of all astrocytes and neurons. Moreover, eGFP was present in the cell body of all Dcx^{+} neurons, while only a small fraction (less than 10%) of astrocytes and of more mature, β-III tubulin[+], neurons lacked somatic eGFP expression. Further analysis, specifically in neuronal processes, revealed robust presence of eGFP in more than 90% of Dcx^{+} cells and in more than 80% of β-III tubulin^{+} cells (**Additional Figure 2D**). Overall, these data confirmed the validity of using these cells in transplantation experiments.

Next, we performed unilateral grafts of 200.000 NPCs[eGFP] just above the SNpc of P45 wild-type mice and killed the animals 3 days post-transplantation (dpt) to check successful graft targeting. We used the contralateral side as internal control and we observed eGFP^{+} cells only at the intended area, in the dorsal margin of the SNpc. A fraction of eGFP^{+} cells had already started to differentiate towards the neuronal or the astroglial lineage, co-expressing Dcx or GFAP, respectively (**Figure 3A** and data not shown).

BNN-20 selectively enhances the midbrain's endogenous neurogenic response after NPC transplantations

We performed similar transplantations in P45 "weaver" mice that had received BNN-20 or vehicle for 15 days (from P30 to P45) and we continued the BNN-20/vehicle administration for another 15 days. The mice were killed at P60, or at P75 (15 and 30 dpt, respectively) (**Figure 3B** and **C**). Before looking at the grafts, we assessed the progress of dopaminergic degeneration, focusing on the contralateral, non-grafted, hemispheres of control mice (that received vehicle) (**Figure 3D**) and we found that the numbers of TH^{+} cells at P75 were almost 1/3rd of those at P60, even though this decrease did not reach statistical significance. This ongoing degeneration was not inhibited or ameliorated by BNN-20 (**Figure 3E**).

Subsequently, we analyzed the grafts, and we observed a reduction in the number of surviving eGFP^{+} cells, at both longer time points, compared with 3 dpt (**Figure 3A–C**). At 3 and 15 dpt, the cells of the graft had not migrated away from the injection site (data not shown). However, at 30 dpt eGFP^{+} cells were detected at distances of more than 500 μm, both ventrally and dorsally, away from the graft (**Figure 3F**). In addition, the morphology of eGFP^{+} cells was different, as they were extending longer and more elaborate processes (**Figure 3G** and **H**). The numbers of surviving eGFP^{+} cells showed high levels of variation between animals at 15 and 30 dpt and were not statistically different with respect to treatment or time ($P > 0.05$, two-way analysis of variance). At both time points, ~5% of transplanted NPCs[eGFP] had acquired a neuronal fate, evident by the expression of Dcx. These neuroblasts were evenly distributed amongst the transplanted cells (**Figure 4A** and **B**) and their percentage did not change significantly from 15 dpt to 30 dpt (**Figure 5A**). Administration of BNN-20 did not affect the neuronal fate of transplanted cells (**Figure 3H**).

The second, more interesting, observation was the emergence of a population of eGFP[−]/Dcx[+] (Dcx^{+}) cells dispersed around the grafts, indicating the recruitment of endogenous neuroblasts (**Figure 4A–C**). The emergence of these cells was dependent on the presence of the graft, as evident by their absence both at the contralateral hemisphere (data not shown) and after a sham procedure in which an identical plan of BNN-20/vehicle administration was followed by the injection of suspension medium only (**Additional Figure 3A** and **B**). The distribution of endogenous neuroblasts at 15 dpt was restricted at a small area around the graft site, varying from 119.23 ± 43.67 to 214.24 ± 56.39 μm away from the injection needle route (**Figure 4C** and **D**). No statistical differences were found between BNN-20 and vehicle-treated mice or between the two directions of migration – towards the midline or laterally (**Figure 4C** and **D**). However, the distribution of these neuroblasts was dramatically expanded, away from the graft, at 30 dpt, with Dcx^{+} cells being detected throughout the whole ipsilateral (left) midbrain area (**Figure 4E**). Notably, their numbers within and adjacent to the site of transplantation were significantly increased from 15 to 30 dpt, irrespective of the administration of BNN-20 (**Figure 5A** and **B**). To assess if the distribution of endogenous neuroblasts coincided with the area directly affected by the graft, we immunostained for GFAP to mark the host tissue domains that reacted to the
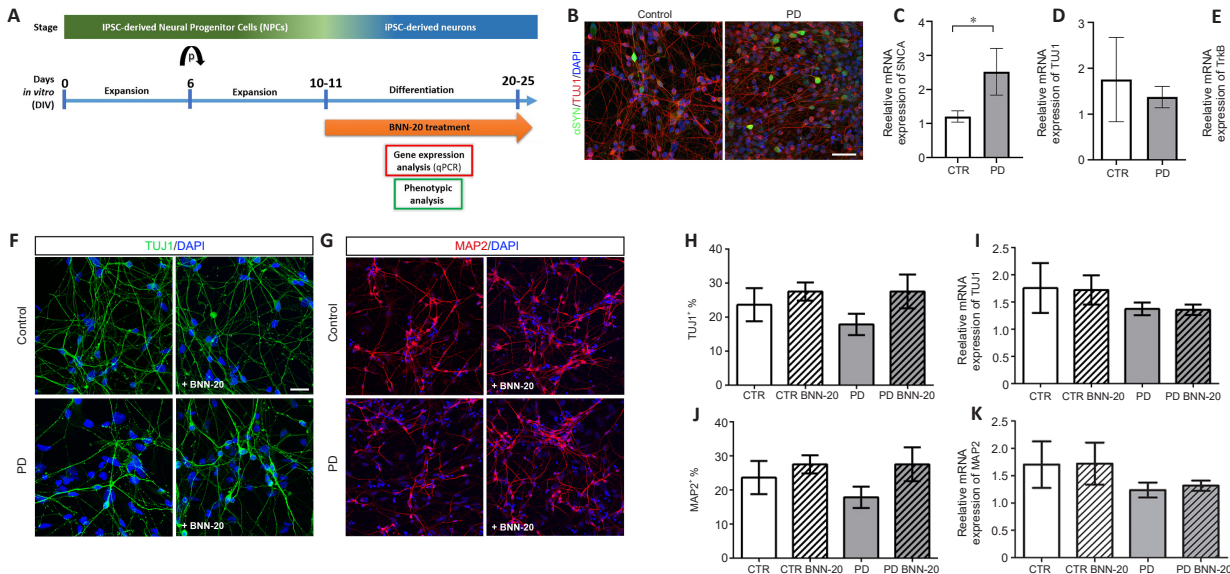
Figure 1 | Effect of BNN-20 on neuronal differentiation of human iPSC-derived NPCs.
(A) Schematic drawing of the protocol used for human iPSC-derived NPC culture and differentiation and timeline of analysis. (B) Immunostaining for α-synuclein (αSyn; green) and βIII-tubulin (TUJ1; red) in control and Parkinson's disease (PD), iPSC-derived neurons at 25 days in vitro (DIV). Cell nuclei are counterstained with DAPI (blue). Scale bar: 50 μm. (C–E) qRT-PCR analysis of α-synuclein gene (SNCA; C), TUJ1 (D), and TrkB (E) mRNA expression normalized to glyceraldehyde-3-phosphate dehydrogenase (GAPDH) levels. Data are represented as mean ± SEM (n = 3). (F, G) Immunostaining for the neuronal markers TUJ1 (green; F) and MAP2 (red; G) in control and PD iPSC-derived neurons at 25 DIV. Cell nuclei are counterstained with DAPI (blue). Scale bars: 20 μm. (H) Graph showing the percentage of TUJ1+/DAPI+ cells. Data are represented as mean ± SEM (n = 3). (I) qRT-PCR analysis of TUJ1 mRNA expression normalized to GAPDH levels. Data are represented as mean ± SEM (n = 3). (J) Graph showing the percentage of MAP2+/DAPI+ cells. Data are represented as mean±SEM (n = 3). (K) qRT-PCR analysis of MAP2 mRNA expression normalized to GAPDH levels. Data are represented as mean ± SEM (n = 3). *P < 0.05 (Student's t-test). BNN-20: Microneurotrophin; Dpt: days post-transplantation; DAPI: 4′,6-diamidino-2-phenylindole; GFAP: glial fibrillary acidic protein; iPSC: induced pluripotent stem cell; MAP2: microtubule-associated protein 2; NPC: neural progenitor cell; qRT-PCR: quantitative reverse transcription-polymerase chain reaction.
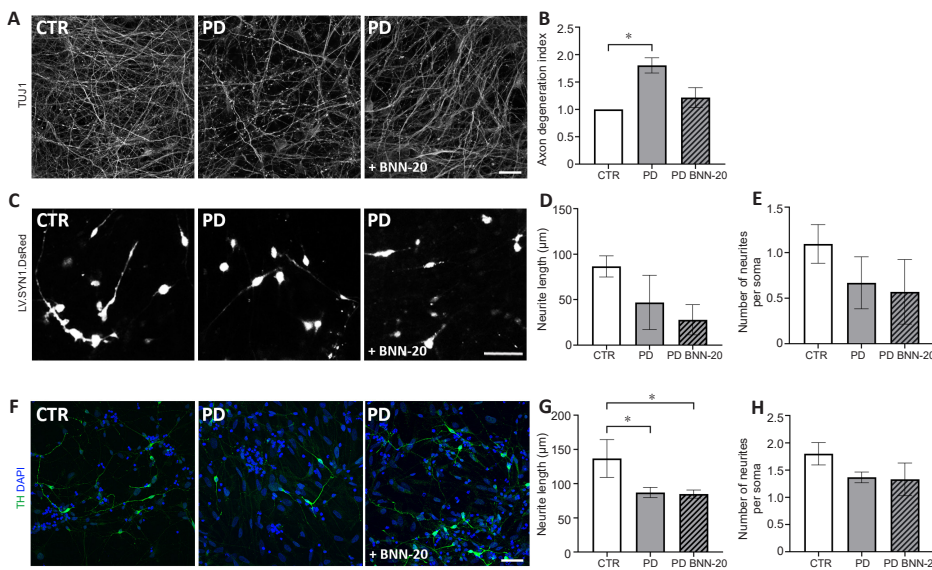

Figure 2 | Effect of BNN-20 on PD-associated phenotypes.
(A) Axonal pathology observed byβIII-tubulin (TUJ1) immunostaining in PD cells at 25 days in vitro (DIV), is slightly improved by BNN-20 treatment. Scale bar: 20 μm. (B) Quantification of neurite degeneration by measuring the ratio of TUJ1+ spots over the total TUJ1+ area in untreated or BNN-20-treated PD iPSC-derived neurons. Data are represented as mean ± SEM (n = 3). (C) Representative fluorescent images of iPSC-derived neurons transduced with LV.SYN1. DsRed. Scale bar: 50 μm. (D, E) Quantification of the total neurite length (D) and neurites extending from the soma (E) in DsRed+ cells. (F) Immunostaining for TH in control and PD untreated and BNN-20-treated iPSC-derived neurons at 25 DIV. Scale bar: 20 μm. (G, H) Quantification of the total neurite length (G) and neurites extending from the soma (H) in TH+ neurons. Data are represented as mean ± SEM (n = at least 70 single DsRed-labeled or TH+ neurons for each condition). *P < 0.05 (one-way analysis of variance with Tukey's post hoc test). BNN-20: Microneurotrophin; dpt: days post-transplantation; iPSC: induced pluripotent stem cell; PD: Parkinson's disease; SNpc: substantia nigra pars compacta; TH: tyrosine hydroxylase; eGFP: enhanced green fluorescent protein.

procedure, at 30 dpt (**Additional Figure 4A–C**). The areas in which activation of astrocytes was observed were not as extended as the areas with emerging Dcx+ cells (compare with **Figure 4E**). Moreover, even though the emergence of Dcx+ neuronal progenitors was dependent, in an obligatory way, on the presence of the graft, their numbers did not correlate with those of surviving eGFP+ cells (Pearson's correlation coefficient r = 0.004 for weaver vehicle-treated mice [wv veh] 15 dpt, r = 0.010 for wv BNN-20 15 dpt, r = 0.231 for wv veh 30 dpt, r = 0.033 for wv BNN-20 30 dpt) (**Figure 5C**). In contrast, as expected, there was a moderate to strong positive correlation between the numbers of graft-derived neuroblasts and of surviving eGFP+ cells (r = 0.369 for wv veh 15 dpt, r = 0.601 for wv BNN-20 15 dpt, r = 0.846 for wv veh 30 dpt, r = 0.900 for wv BNN-20 30 dpt; **Figure 5C**).

Importantly, when the pro-neurogenic capacity of the transplants was measured as the ratio of emerging neuroblasts per eGFP+ cells (referred to from now on as "graft efficiency"), it was found to be significantly increased by BNN-20 (**Figure 5B**). The graft efficiency was increased after BNN-20 administration at 30 dpt, compared with both vehicle animals and to 15 dpt, for the endogenous (Dcx+/eGFP−) but not the exogenous (Dcx+/eGFP+) neuroblasts (**Figure 5B**). If in our calculations we add all neuroblasts

(endogenous and graft-derived), then the total neurogenic capacity of the grafts is even more strongly enhanced by BNN-20 administration (**Figure 5B**).

Despite the extensive presence of Dcx+ cells inside and outside the SNpc at 30 dpt, the number of TH+ cells in the grafted hemispheres was similar to those in the contralateral sides, irrespective of BNN-20 administration (**Figure 3E**). Only one example of a graft-derived dopaminergic neuron (TH+/eGFP+) was observed in the SNpc proximal to the site of transplantation (**Figure 3I**) and expression of FoxA2 was not detected at the proximity of the graft. However, to further investigate the background of the expanded distribution of Dcx+ cells at 30 dpt, we explored the response of endogenous progenitor populations by counting the numbers of Sox2+ NPCs, of GFAP+/Sox2+ reactive glia and of FoxA2+ dopaminergic progenitors in the SNpc, at 15 dpt, before the emergence of the neuroblasts' expansion wave (**Additional Figure 5A and B**). We found no differences in the density of Sox2+ progenitors after BNN-20 administration, but we detected a statistically significant decrease in the density of GFAP+/Sox2+ cells only in response to the combination of graft and BNN-20, compared with all other experimental groups. Moreover, the number of cells expressing FoxA2, but being negative for TH, was increased in both hemispheres after BNN-20 administration (**Additional Figure 5C–E**).
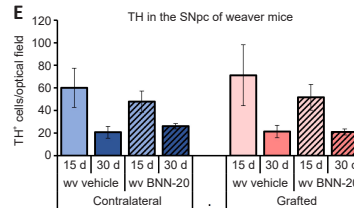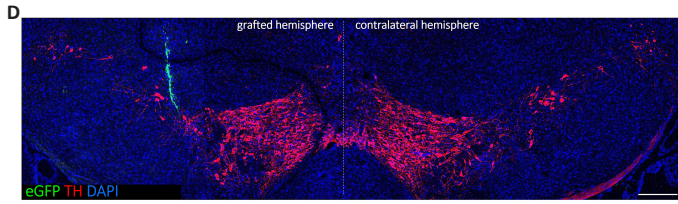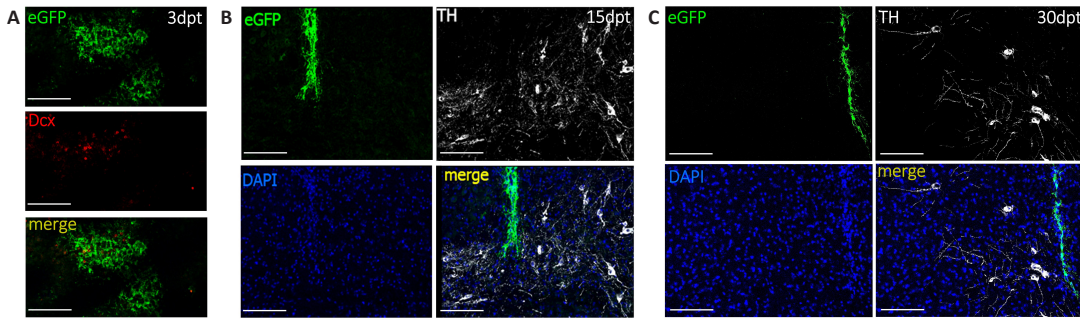
Figure 3 | Evaluation of the viability and differentiation of the grafted cells, and of the effect of BNN-20 + graft treatment on the "weaver" substantia nigra.

(A–C) Representative immunofluorescence images of the graft site at 3 days post-transplantation (dpt; A), 15 dpt (B) & 30 dpt (C). (B, C) The grafted cells (eGFP+) were placed right above the dorsal margin of the SNpc (TH+ dopaminergic neurons in white). (D) Representative collage of immunofluorescence images depicting the dopaminergic neurons (TH+, red) of the SNpc of a transplanted weaver mouse (eGFP+ cells in green) at 30 dpt. The SNpc contralateral to the graft was used as an internal control. (E) Dopaminergic degeneration showed a trend for further deterioration from postnatal day 60 (P60–15 dpt) to P75 (30 dpt), irrespective of the group. No effect of the graft treatment was observed on the number of dopaminergic neurons of the SNpc. Error bars are SEMs. Statistical analysis was performed using Student's t-test (n = 3). (F, G) Immunofluorescence images depicting the significant rostral-caudal and dorsoventral migration (F), as well as the branching of the grafted (eGFP+) cells (G), observed at 30 dpt compared with 3 and 15 dpt. The dotted areas depict examples of highly branched graft-derived (eGFP+) cells, including Dcx+ neuroblasts, that have migrated from the injection site. (H) Histogram and representative images of graft-derived neuroblasts (Dcx+/eGFP+) at the site of the graft. The left panel shows the characteristic morphology of the graft-derived neuroblasts at 30 dpt. The arrowheads indicate a representative example of a graft-derived neuroblast with long-extending cellular processes. No significant changes were observed between groups. Statistical analysis was performed using one-way analysis of variance (n = 4 animals per group for 15 dpt and n = 3 animals per group for 30 dpt). Error bars are SEMs. (I) Only one TH+/eGFP+ (graft-derived) dopaminergic neuron was observed at 30 dpt in the ipsilateral SNpc. Scale bars: 116 μm in A–C, 232 μm in D, F (low magnification collages) 58 μm in F1–F4 insets, 58 μm in H, 14 μm in I. BNN-20: Microneurotrophin; dpt: days post-transplantation; SNpc: substantia nigra pars compacta; TH: tyrosine hydroxylase; eGFP: enhanced green fluorescent protein.
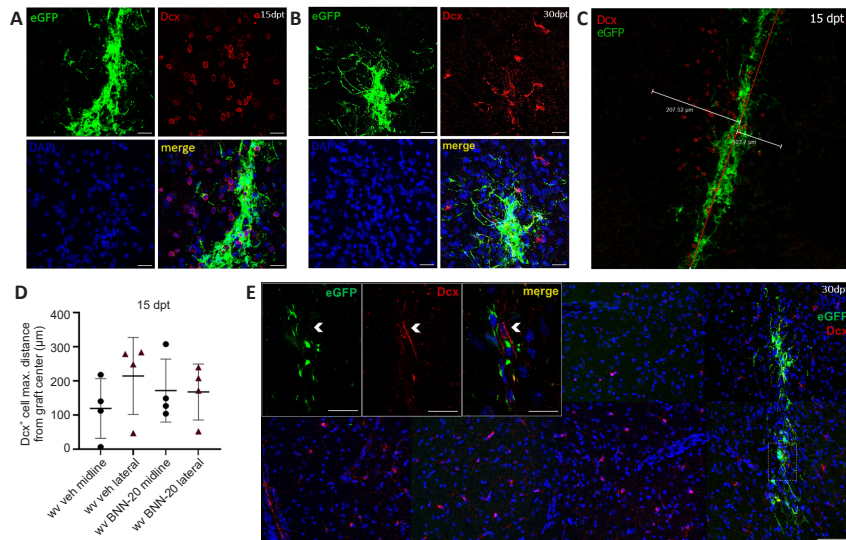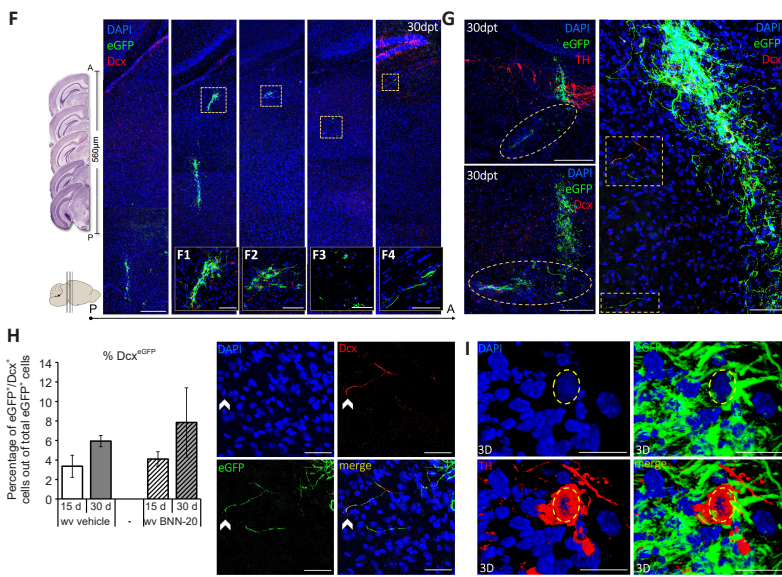

Figure 4 | Distribution of the endogenous pool of neuroblasts appearing after BNN-20 + graft treatment in the ipsilateral to the graft hemisphere.

(A) Representative immunofluorescence images depicting the appearance of a significant number of Dcx+/eGFP− (endogenous) neuroblasts adjacent to the site of the graft at 15 dpt. (B) After 30 dpt the aforementioned cells present a different, more typical morphology, with long cellular processes extending from the soma. (C, D) Distribution of these endogenous (Dcx+/eGFP−) neuroblasts at 15 dpt: (C) Method for quantification of the maximum distance where Dcx+/eGFP− cells were found from the needle tract (graft center), (D) Dot plot depicting the distribution of the Dcx+/eGFP− neuroblasts towards two directions (towards the midline and laterally) from the graft center. Statistical analysis was performed with one-way analysis of variance, n = 4 samples per group. (E) Moreover, the distribution of the endogenous (Dcx+/eGFP−) neuroblasts expanded at 30 dpt compared with 15 dpt, covering the whole ipsilateral to the graft midbrain area. The panel on the left upper corner is a magnified (40×) inset of one optical plane of the area outlined by the dashed square (appearing with maximized signal, magnification 20×). Scale bars: 53 μm in A and B; 58 μm in C and E (main figure), 15 μm in inset in E. BNN-20: Microneurotrophin; dpt: days post-transplantation; eGFP: enhanced green fluorescent protein.
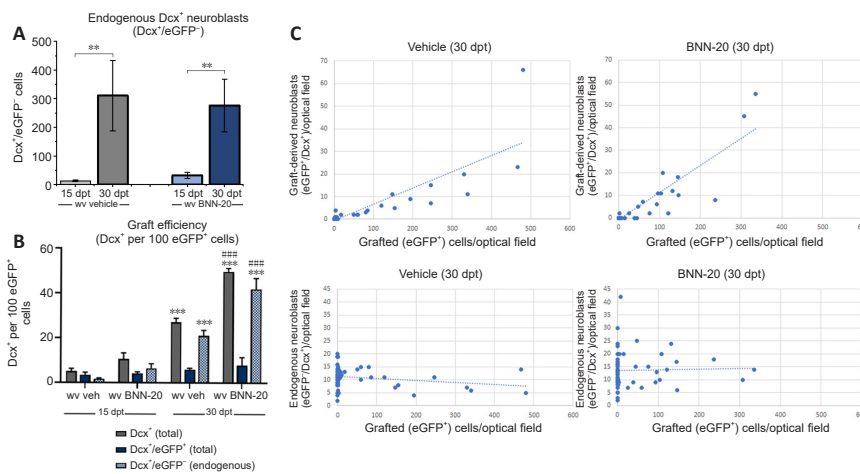
Figure 5 | Quantifications and correlation analysis of the neuroblast populations appearing after BNN-20 + graft treatment in the ipsilateral to the graft hemisphere.
(A) Histogram depicting the total numbers of Dcx$^+$/eGFP$^-$ endogenous neuroblasts, significantly increased from 15 dpt to 30 dpt irrespective of BNN-20 administration. Data are represented as mean ± SEM. Statistical comparisons were performed with one-way analysis of variance with Bonferroni correction (n = 4 animals per group for 15 dpt and n = 3 animals per group for 30 dpt). (B) Histogram depicting the neurogenic efficiency of the graft, expressed as the ratio of Dcx$^+$ cell subpopulations per 100 eGFP$^+$ cells, significantly enhanced by BNN-20 administration. n = 4 animals per group for 15 dpt and n = 3 animals per group for 30 dpt. Data are represented as mean ± SEM. **$P < 0.05$, ***$P < 0.001$, $vs.$ 15 dpt; ###$P < 0.001$, $vs.$ wv veh 30 dpt (one-way analysis of variance with Bonferroni correction). (C) Scatter plots depicting the correlation between the surviving grafted cells and the Dcx$^+$ subpopulations. There is a moderate to strong positive correlation (r = 0.369 for weaver [wv] vehicle [veh] 15 dpt, r = 0.601 for wv BNN-20 15 dpt, r = 0.846 for wv veh 30 dpt, r = 0.900 for wv BNN-20 30 dpt) between the emergence of graft-derived (Dcx$^+$/eGFP$^+$), but not of endogenous (Dcx$^+$/eGFP$^-$) neuroblasts with the total surviving grafted cells (eGFP$^+$) at 30 dpt. Statistical analysis was performed using Pearson's correlation analysis (n = 4 animals per group for 15 dpt and n = 3 animals per group for 30 dpt). BNN-20: Microneurotrophin; dpt: days post-transplantation; eGFP: enhanced green fluorescent protein.

Discussion

The use of NPC transplantations as a therapeutic strategy in PD is currently under intense investigation (Hiller et al., 2022). The beneficial effects of stem/progenitor cell grafts in the brain can be exerted via direct replacement, or via modulation of the host's microenvironment and the activation of endogenous progenitors (Mine et al., 2013; Ryu et al., 2016); although the latter is rarely investigated. Previous results have demonstrated the existence of low-rate endogenous neurogenesis in the SNpc of wild-type and weaver mice that can be induced by the early postnatal administration of the microneurotrophin BNN-20, leading to a partial reversal of degeneration (Mourtzi et al., 2021). Here we examined the effects of an intranigral NPC graft and of BNN-20 administration, alone or concurrently, in the "weaver" mouse. One first, surprising, result was that the administration of the microneurotrophin (P30–P60 or P30–P75) was ineffective in terms of dopaminergic neuroprotection/regeneration. This was unforeseen, since previous results clearly demonstrated that BNN-20 had a neuroprotective/pro-neurogenic effect during earlier stages of nigrostriatal degeneration (e.g., P14–P40, P14–P60 or P20–P60), not only inhibiting further degeneration but, in some cases, even increasing the number of dopaminergic neurons when compared with the point of initiation (Panagiotakopoulou et al., 2020; Mourtzi et al., 2021). This finding suggests that BNN-20 exhibits a narrower than what we estimated window of opportunity for the protection and/or replacement of dopaminergic neurons in the "weaver" SNpc. This could be due to a continued deterioration of the SNpc microenvironment, as revealed by the fact that dopaminergic degeneration progressed further from P60 to P75, leaving the SNpc even more severely hypocellularized. Because neuroinflammation and increased levels of oxidative stress are the most probable culprits for this deterioration and since BNN-20 has been shown to efficiently target both these processes at earlier stages, it would be desirable to investigate if longer periods or higher doses of BNN-20 administration, could be beneficial at phases of degeneration that are compatible with the late stages of human PD.

A low-level neurogenic activity within the SNpc, which is not enhanced in the "weaver" brain and which involves dopaminergic lineage progenitors (marked by FoxA2 expression) has been recently reported (Mourtzi et al., 2021). Here, we confirmed the absence of Dcx$^+$ neuroblasts in the weaver SNpc or in the rest of the midbrain area. This is in contrast to other types of neurodegeneration, such as ischemic stroke, that lead to the activation of local quiescent progenitors both in animal models (Zamboni et al., 2020; Simões et al., 2022) and in humans (Ernst et al., 2014) and can induce the migration of neuroblasts from distant niches (Thored et al., 2007; Grade et al., 2013; Dillen et al., 2020). In cases of chronic degeneration, resulting in hostile and fallow brain microenvironments, such as the "weaver" mouse, cell transplantations were considered to be the sole option to achieve some level of regeneration. In our experiments, the grafts failed to improve the SNpc histopathology. Transplanted cells were gradually depleted, and showed restricted migratory potential and a low neurogenic capacity (approximately 5% of cells expressed Dcx) with no substantial evidence of dopaminergic cell replacement. On the other hand, we documented clear evidence of increased cell mobility between 15 and 30 dpt, complemented by improved cell morphology (e.g., extension of processes), observations that warrant further investigation at longer time points.

The first key finding of this study was the induction of neurogenic activity by the grafts, evidenced by the emergence of endogenous neuroblasts after the 3 dpt time-point and by the appearance of Sox2$^+$ cells near the graft (Ellis et al., 2004). Although similar results have been described previously, for example in transplantation experiments in animal models of stroke (Mine et al., 2013; Ryu et al., 2016) and in the striatum of the 6-OHDA PD model (Madhavan et al., 2009), implicating molecular pathways such as Notch signaling (Llorens-Bobadilla et al., 2015; Magnusson et al., 2020; Santopolo et al., 2020), this is the first detailed investigation of such an effect in the weaver mouse. The number of endogenous neuroblasts increased significantly from 15 to 30 dpt around the graft, in parallel with the appearance of Dcx$^+$ cells farther away, in several midbrain areas, including the SNpc. As with the cells of the graft, the morphology of these neuroblasts became more elaborate over time, indicating increased levels of maturity (Schörnig et al., 2021) and a level of resistance to the hostile microenvironment of the tissue, that has been described for endogenously newborn neurons at earlier stages of degeneration (Mourtzi et al., 2021). Importantly, the size and distribution of the pool of neuroblasts were not proportional to that of eGFP$^+$ cells, or the distribution of gliosis, suggesting that at these post-transplantation phases of endogenous neurogenesis had become independent of the graft. The massive expansion of the area in which endogenous neuroblasts were detected at 30 dpt needs further investigation. Our approach does not allow us to assess if these are cells gradually migrating from the area of the graft, or if they emerge locally, indicating a gradual expansion of the area permissive for neurogenesis. The observation that their distribution does not correlate with the migratory behavior of grafted cells points toward the second scenario.

Our second key result was that the administration of BNN-20 significantly enhanced the neurogenic capacity of the grafts, as judged by the increased ratio of emerging neuroblasts per eGFP$^+$ cells. To our knowledge, this is the first report of a substance acting in combination with an NPC graft to enhance directly and specifically endogenous neurogenesis. BNN-20 also led to an increase in the numbers of endogenous dopaminergic progenitors (FoxA2$^+$/TH$^-$/eGFP$^-$ cells) in the SNpc. It remains elusive whether BNN-20 exerts its effects by boosting the stimulatory activity of transplanted NPCs, by increasing the responsiveness of endogenous progenitors, or both. Our current results, together with previous results have shown: i) limited effects of BNN-20 on human and mouse NPCs $in vitro$; ii) direct effects on endogenous SNpc-specific neurogenesis (Mourtzi et al., 2021), and iii) a gradual independence of endogenous neurogenesis from the grafted cells. Moreover, BNN-20 shifts the polarization of microglia from the proapoptotic M1 towards the neuroprotective M2 phenotype, acting as a beneficial immunomodulator (Panagiotakopoulou et al., 2020) and exhibits antioxidant and antiapoptotic properties (Botsakis et al., 2017). Overall, these data indicate a mode of activity that involves multiple cell types, besides NPCs, leading to an improved tissue microenvironment that is consistent with a pro-neurogenic effect (Yuan et al., 2015; Araki et al., 2021).

Another finding, specific to the "graft+BNN-20" combinatory intervention, was the significant decrease in the numbers of double GFAP$^+$/Sox2$^+$ cells, that we consider to be reactive astrocytes. Several reports indicate that gliosis (leading to the formation of a glial scar) could represent a "stumbling block" resulting in a poor stem cell transplantation outcome and/or the inhibition of endogenous reparative mechanisms of the adult brain (Robel et al., 2011; Gerlach et al., 2016; Pekny et al., 2019). It has been proposed that NPC transplantations attenuate the formation of the glial scar and that BDNF may have the same effect, alone or in combination with mesenchymal stem cell transplantations, anti-inflammatory peptides, or advanced biomaterials (Hassannejad et al., 2019; He et al., 2019; Chang et al., 2021). Since BNN-20 is a BDNF-mimicking molecule (Botsakis et al., 2017; Panagiotakopoulou et al., 2020), our results are compatible with the activation of a stronger anti-gliotic BDNF signaling pathway when BNN-20 is combined with the NPC graft.

Finally, we exposed human iPSC-derived NPCs, generated from PD patients and unaffected donors to BNN-20 for two reasons. On one hand, these cells can be used to model human pathology, with our results reinforcing and expanding previous observations (Kouroupi et al., 2017) as we identified pathological traits after short-term spontaneous differentiation of the PD-derived cells, and also can be used as a potential resource for transplantation strategies. The effects of BNN-20 were limited on these cells $in vitro$, as it exhibited a marginal pro-neurogenic activity and only partially alleviated pathological traits. The lack of stronger effects could reflect the differences

between human and rodent NPCs but, at this stage, does not preclude the therapeutic potential of BNN-20. Additional experiments in human and animal cells are necessary to identify other possible effects of BNN-20 and to expand our knowledge of the pathways underlying BNN-20's activity. For example, the iPSC differentiation protocol used in this study is mostly relevant to developmental rather than adult neurogenic pathways, and BNN-20 has been so far shown to be effective only in the latter.

This study has some limitations that should be noted. First of all, due to the increased morbidity and mortality of the "weaver" mouse strain, we could only follow up the grafted NSPCs, as well as the graft-induced newborn neuroblasts for 30 days post-transplantation. However, there is a chance that more time is needed for the graft-derived neuroblasts to fully differentiate and migrate to their final destination, including the SNpc. The latter could explain the lack of graft-derived dopaminergic neurons in the SNpc, except for only one example of such a neuron. Using another model of PD could allow a longer follow-up in the future, to investigate this hypothesis. Moreover, although we have clearly demonstrated the graft-induced appearance of endogenous Dcx⁺ neuroblasts around the site of transplantation (that is completely absent in the contralateral hemisphere (where no surgical intervention took place), as well as in a sham experimental group (where only dispersion medium was stereotaxically injected in the same coordinates), and their vast increase and propagation in a time-dependent manner (from 15 to 30 days post); we did not have the chance to investigate their exact origin or their specific cell fate. Cell tracking experiments (e.g., with the use of transgenic animals expressing fluorescent dyes under the control of the Dcx promoter) could provide significant answers to this question in the future. Last but not least, for the *in vivo* experiments, we selected to work with a single BNN-20 dosage of 100 mg/kg b.w., based on previous knowledge of the neuroprotective/pro-neurogenic effect of the microneurotrophin in "weaver" mice. However, as we have initiated BNN-20's administration at a later time-point (of greater dopaminergic degeneration and probably a more hostile microenvironment), higher doses of BNN-20 could possibly produce better results. Hence, it could be valuable to evaluate this in the future.

In conclusion, the data we report here show that BNN-20 has limited direct effects on cultured human iPSC-derived NPCs and grafted mouse NPCs. However, it strongly enhances the transplantation-induced endogenous neurogenesis in the midbrain. These results provide further and clear evidence of the existence of an endogenous midbrain neurogenic system that can be specifically strengthened by BNN-20. The activation of endogenous neurogenesis in the weaver mouse midbrain (even outside the SNpc that retains a continuous low-level neurogenic activity), which is directly dependent on the graft and significantly enhanced by BNN-20, is a significant first step in the direction of assessing the benefits of manipulating endogenous, dormant, neural progenitors to boost the regeneration of the depleted SNpc. This becomes more important in light of accumulating recent evidence showing that the reprogramming of endogenous cells offers a therapeutic target possibly superior to other cell-based approaches as newborn neurons can establish satisfactory nigrostriatal connections.

Additional files:
Additional Figure 1: Schematic depiction of the timeline of interventions, used for the transplantation experimental protocols.
Additional Figure 2: In vitro characterization of eGFP expression and differentiation potential of the NPCs^eGFP [C57BL/6-Tg (CAG-eGFP)1Osb/J] used for transplantations.
Additional Figure 3: Emergence of an endogenous neuroblast population (Dcx⁺/eGFP⁻) in the ipsilateral to the graft hemisphere versus a sham surgical procedure.
Additional Figure 4: GFAP and Sox2 expression throughout the brain of unilaterally grafted weaver mice at 30 dpt.
Additional Figure 5: Analysis of the expression of dopaminergic (TH, FoxA2), astrocytic (GFAP), and neural stem/progenitor (Sox2) cell markers in the SNpc of grafted weaver mice.
Additional file 1: Supplementary information on the Materials and Methods.

References

Araki T, Ikegaya Y, Koyama R (2021) The effects of microglia- and astrocyte-derived factors on neurogenesis in health and disease. Eur J Neurosci 54:5880-5901.

Botsakis K, Mourtzi T, Panagiotakopoulou V, Vreka M, Stathopoulos GT, Pediaditakis I, Charalampopoulos I, Gravanis A, Delis F, Antoniou K, Zisimopoulos D, Georgiou CD, Panagopoulos NT, Matsokis N, Angelatou F (2017) BNN-20, a synthetic microneurotrophin, strongly protects dopaminergic neurons in the "weaver" mouse, a genetic model of dopamine-denervation, acting through the TrkB neurotrophin receptor. Neuropharmacology 121:140-157.

Chambers SM, Fasano CA, Papapetrou EP, Tomishima M, Sadelain M, Studer L (2009) Highly efficient neural conversion of human ES and iPS cells by dual inhibition of SMAD signaling. Nat Biotechnol 27:275-280.

Chang DJ, Cho HY, Hwang S, Lee N, Choi C, Lee H, Hong KS, Oh SH, Kim HS, Shin DA, Yoon YW, Song J (2021) Therapeutic effect of BDNF-overexpressing human neural stem cells (F3.BDNF) in a contusion model of spinal cord injury in rats. Int J Mol Sci 22:6970.

Dillen Y, Kemps H, Gervois P, Wolfs E, Bronckaers A (2020) Adult neurogenesis in the subventricular zone and its regulation after ischemic stroke: implications for therapeutic approaches. Transl Stroke Res 11:60-79.

Duda JE, Giasson BI, Mabon ME, Lee VMY, Trojanowski JQ (2002) Novel antibodies to synuclein show abundant striatal pathology in Lewy body diseases. Ann Neurol 52:205-210.

Ellis P, Fagan BM, Magness ST, Hutton S, Taranova O, Hayashi S, McMahon A, Rao M, Pevny L (2004) SOX2, a persistent marker for multipotential neural stem cells derived from embryonic stem cells, the embryo or the adult. Dev Neurosci 26:148-165.

Ernst A, Alkass K, Bernard S, Salehpour M, Perl S, Tisdale J, Possnert G, Druid H, Frisen J (2014) Neurogenesis in the striatum of the adult human brain. Cell 156:1072-1083.

Gerlach J, Donkels C, Münzner G, Haas CA (2016) Persistent gliosis interferes with neurogenesis in organotypic hippocampal slice cultures. Front Cell Neurosci 10:131.

Grade S, Weng Y, Snapyan M, Kriz J, Malva JO, Saghatelyan A (2013) Brain-derived neurotrophic factor promotes vasculature-associated migration of neuronal precursors toward the ischemic striatum. PLoS One 8:e55039.

Hassannejad Z, Zadegan SA, Vaccaro AR, Rahimi-Movaghar V, Sabzevari O (2019) Biofunctionalized peptide-based hydrogel as an injectable scaffold for BDNF delivery can improve regeneration after spinal cord injury. Injury 50:278-285.

He Z, Zang H, Zhu L, Huang K, Yi T, Zhang S, Cheng S (2019) An anti-inflammatory peptide and brain-derived neurotrophic factor-modified hyaluronan-methylcellulose hydrogel promotes nerve regeneration in rats with spinal cord injury. Int J Nanomedicine 14:721-732.

Hiller BM, Marmion DJ, Thompson CA, Elliott NA, Federoff H, Brundin P, Mattis VB, McMahon CW, Kordower JH (2022) Optimizing maturity and dose of iPSC-derived dopamine progenitor cell therapy for Parkinson's disease. NPJ Regen Med 7:24.

Hirano A, Dembitzer HM (1973) Cerebellar alterations in the weaver mouse. J Cell Biol 56:478-486.

Kouroupi G, Taoufik E, Vlachos IS, Tsioras K, Antoniou N, Papastefanaki F, Chroni-Tzartou D, Wrasidlo W, Bohl D, Stellas D, Politis PK, Vekrellis K, Papadimitriou D, Stefanis L, Bregestovski P, Hatzigeorgiou AG, Masliah E, Matsas R (2017) Defective synaptic connectivity and axonal neuropathology in a human iPSC-based model of familial Parkinson's disease. Proc Natl Acad Sci U S A 114:E3679-3688.

Llorens-Bobadilla E, Zhao S, Baser A, Saiz-Castro G, Zwadlo K, Martin-Villalba A (2015) Single-cell transcriptomics reveals a population of dormant neural stem cells that become activated upon brain injury. Cell Stem Cell 17:329-340.

Madhavan L, Daley BF, Paumier KL, Collier TJ (2009) Transplantation of subventricular zone neural precursors induces an endogenous precursor cell response in a rat model of Parkinson's disease. J Comp Neurol 515:102-115.

Magnusson JP, Zamboni M, Santopolo G, Mold JE, Barrientos-Somarribas M, Talavera-Lopez C, Andersson B, Frisén J (2020) Activation of a neural stem cell transcriptional program in parenchymal astrocytes. eLife 9:e59733.

Marsh SE, Blurton-Jones M (2017) Neural stem cell therapy for neurodegenerative disorders: The role of neurotrophic support. Neurochem Int 106:94-100.

Mendez I, Dagher A, Hong M, Hebb A, Gaudet P, Law A, Weerasinghe S, King D, Desrosiers J, Darvesh S, Acorn T, Robertson H (2000) Enhancement of survival of stored dopaminergic cells and promotion of graft survival by exposure of human fetal nigral tissue to glial cell line-derived neurotrophic factor in patients with Parkinson's disease. Report of two cases and technical considerations. J Neurosurg 92:863-869.

Mine Y, Tatarishvili J, Oki K, Monni E, Kokaia Z, Lindvall O (2013) Grafted human neural stem cells enhance several steps of endogenous neurogenesis and improve behavioral recovery after middle cerebral artery occlusion in rats. Neurobiol Dis 52:191-203.

Mourtzi T, Kazanis I (2022) Endogenous versus exogenous cell replacement for Parkinson's disease: where are we at and where are we going? Neural Regen Res 17:2637-2642.

Mourtzi T, Dimitrakopoulos D, Kakogiannis D, Salodimitris C, Botsakis K, Meri DK, Anesti M, Dimopoulou A, Charalampopoulos I, Gravanis A, Matsokis N, Angelatou F, Kazanis I (2021) Characterization of substantia nigra neurogenesis in homeostasis and dopaminergic degeneration: beneficial effects of the microneurotrophin BNN-20. Stem Cell Res Ther 12:335.

Panagiotakopoulou V, Botsakis K, Delis F, Mourtzi T, Tzatzarakis MN, Dimopoulou A, Poulia N, Antoniou K, Stathopoulos GT, Matsokis N, Charalampopoulos I, Gravanis A, Angelatou F (2020) Anti-neuroinflammatory, protective effects of the synthetic microneurotrophin BNN-20 in the advanced dopaminergic neurodegeneration of "weaver" mice. Neuropharmacology 165:107919.

Paxinos G, Franklin KBJ (2013) Paxinos and Franklin's the mouse brain in stereotaxic coordinates. 4ᵗʰ ed. Boston: Elsevier/Academic Press.

Pekny M, Wilhelmsson U, Tatlisumak T, Pekna M (2019) Astrocyte activation and reactive gliosis—A new target in stroke? Neurosci Lett 689:45-55.

Percie du Sert N, Hurst V, Ahluwalia A, Alam S, Avey MT, Baker M, Browne WJ, Clark A, Cuthill IC, Dirnagl U, Emerson M, Garner P, Holgate ST, Howells DW, Karp NA, Lazic SE, Lidster K, MacCallum CJ, Macleod M, Pearl EJ, et al. (2020) The ARRIVE guidelines 2.0: Updated guidelines for reporting animal research. PLoS Biol 18:e3000410.

Robel S, Berninger B, Götz M (2011) The stem cell potential of glia: lessons from reactive gliosis. Nat Rev Neurosci 12:88-104.

Ryu S, Lee SH, Kim SU, Yoon BW (2016) Human neural stem cells promote proliferation of endogenous neural stem cells and enhance angiogenesis in ischemic rat brain. Neural Regen Res 11:298-304.

Santopolo G, Magnusson JP, Lindvall O, Kokaia Z, Frisén J (2020) Blocking Notch-signaling increases neurogenesis in the striatum after stroke. Cells 9:1732.

Schmittgen TD, Livak KJ (2008) Analyzing real-time PCR data by the comparative CT method. Nat Protoc 3:1101-1108.

Schneider CA, Rasband WS, Eliceiri KW (2012) NIH Image to ImageJ: 25 years of image analysis. Nat Methods 9:671-675.

Schörnig M, Ju X, Fast L, Ebert S, Weigert A, Kanton S, Schaffer T, Nadif Kasri N, Treutlein B, Peter BM, Hevers W, Taverna E (2021) Comparison of induced neurons reveals slower structural and functional maturation in humans than in apes. eLife 10:e59323.

Simões AR, Neto M, Alves CS, Santos MB, Fernández-Hernández I, Veiga-Fernandes H, Brea D, Durá I, Encinas JM, Rhiner C (2022) Damage-responsive neuro-glial clusters coordinate the recruitment of dormant neural stem cells in Drosophila. Dev Cell 57:1661-1675.e1667.

Thored P, Wood J, Arvidsson A, Cammenga J, Kokaia Z, Lindvall O (2007) Long-term neuroblast migration along blood vessels in an area with transient angiogenesis and increased vascularization after stroke. Stroke 38:3032-3039.

Yuan TF, Gu S, Shan C, Marchado S, Arias-Carrión O (2015) Oxidative stress and adult neurogenesis. Stem Cell Rev Rep 11:706-709.

Zamboni M, Llorens-Bobadilla E, Magnusson JP, Frisén J (2020) A widespread neurogenic potential of neocortical astrocytes is induced by injury. Cell Stem Cell 27:605-617.e605.

C-Editors: Zhao M, Liu WJ; S-Editor: Li CH; L-Editors: Li CH, Song LP; T-Editor: Jia Y